International Journal of Applied Mathematics
Volume 38 No. 5s, 2025
ISSN: 1311-1728 (printed version); ISSN: 1314-8060 (on-line version)

COMPARATIVE ASSESSMENT OF VARIANTS OF SIMULTANEOUS ALGEBRAIC RECONSTRUCTION TECHNIQUE WITH PROPOSED HYBRID FILTERED BACK PROJECTION ALGORITHM

Ravi Krishan Pandey[1], Praveen K Shukla[2], Dharmendra Lal Gupta[3]

[1, 2] *Babu Banarasi Das University, Lucknow, India.*

[3] *Kamla Nehru Institute of Technology, Sultanpur, India.*

Email id- profravikp@gmail.com, drpraveenkumarshukla@gmail.com, dlgupta2002@gmail.com.

Abstract

Introduction: This paper introduces a novel hybrid approach to computed tomography (CT) image reconstruction, designed to enhance medical imaging techniques. The study meticulously compares the performance of this innovative method with established algorithms, including back projection, simultaneous algebraic reconstruction (SAR), and simultaneous algebraic reconstruction iteration (SART) coupled with a total variation minimization algorithm. The evaluation utilizes the NIH-AAPM-Mayo Clinic CT Grand Challenge dataset, ensuring robust and relevant results. Two key performance metrics are taken for comparison: the Structural Similarity Index Measure (SSIM) and the Peak Signal-to-Noise Ratio (PSNR).

Objectives: To enhance the quality of filtered back projection (FBP) images in low-dose imaging,

Methods: A hybrid model is proposed and compared with SART variants. It combines FBP with a modified CNN featuring three 2D convolution layers (32, 64, and 128 filters of size 3x3) and a ReLU activation function, with an input shape of 150x150 in a batch size of 8. Three 2D max-pooling layers with 2x2 kernel sizes are included. The output is flattened and passed through a dense layer (128 units, ReLU activation), followed by a dropout layer (0.5) to reduce overfitting. The final dense layer uses Softmax for activation. The model is compiled with categorical cross-entropy the loss function and the ADAM as optimizer. Training occurs on a machine with an NVIDIA GEFORCE RTX GPU (6 GB memory).

Results: The hybrid algorithm achieved an SSIM value of 0.7916, indicating superior structural fidelity in reconstructed images. Additionally, it demonstrated a PSNR of 19.0424 dB, confirming its effectiveness in producing higher-quality images.

Conclusions: The findings have crucial implications for medical imaging, promoting safer practices to reduce radiation exposure by enhancing image quality. This balance between quality and safety highlights the significance of the research, which could revolutionize diagnostic methods in healthcare. Overall, it represents a pivotal advancement in hybrid CT reconstruction, paving the way for further innovations in medical imaging technologies.

Keywords: computed tomography, image reconstruction, filtered back projection, iterative reconstruction, simultaneous algebraic reconstruction technique, convolutional neural network.

Received: August 08, 2025

International Journal of Applied Mathematics
Volume 38 No. 5s, 2025
ISSN: 1311-1728 (printed version); ISSN: 1314-8060 (on-line version)

Introduction

Medicine has advanced significantly in recent decades due to improvements in diagnostic techniques. These faster and more accurate methods allow doctors to provide targeted treatments for specific diseases, encompassing pathological and imaging techniques. CT is an essential medical imaging technique widely utilized in healthcare. A CT scan, leveraging advanced X-ray technology, effectively generates detailed cross-sectional images of bones, soft tissues, and organs. Unlike traditional X-rays that use a fixed tube, a CT scanner has a motorized X-ray source that emits narrow beams while rotating around the patient. Digital detectors capture these X-rays and send the data to a computer, creating tomographic images. These images can be displayed in two dimensions or combined into a three-dimensional format, aiding physicians in identifying abnormalities and guiding treatment planning. (Griffin, J., 2022). [1]

CT image reconstruction techniques have advanced significantly to diminish radiation exposure while upholding high image quality. Traditional methods like Filtered Back Projection (FBP) and Iterative Reconstruction (IR) remain foundational, but current advancements in Artificial Intelligence (AI) and Deep Learning (DL) have improved noise suppression, artifact reduction, and structure preservation. These modern techniques are useful in low-dose CT applications, balancing image quality, computational efficiency, and adaptability. (Ikuta & Zhang, 2023). [2] Below, the key CT image reconstruction techniques are discussed.

- Filtered Back Projection (FBP): A widely used and standard analytical method that has been used for decades for reconstructing images by back-projecting filtered projection data. It is fast but often results in high noise levels, especially in low-dose scenarios (Koetzier et al., 2023) (Cong, W. et al., 2024). [3] [4] It transforms the fresh data acquired from a CT scanner (sinogram images) into cross-sectional images. The Radon transform is a key component of FBP, converting CT slice data into a sinogram for reconstruction (Wright, 2022). [5] A comparison between the results of BP & FBP for CT image reconstruction is shown in the figure below (Vamvakeros, A., 2017). [6]

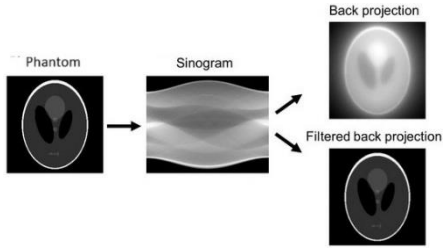

Figure 1 Comparison of BP and FBP

- Iterative Reconstruction (IR): This method refers to a set of algorithms used to reconstruct 2D and 3D images in various imaging techniques, such as CT, Magnetic Resonance Imaging (MRI), and Synthetic-Aperture Radar (SAR). Iterative Reconstruction (IR) techniques refine images through multiple iterations, minimizing the difference between measured and estimated projections. While IR enhances image quality compared to Filtered

Received: August 08, 2025

ISSN: 1311-1728 (printed version); ISSN: 1314-8060 (on-line version)

Back Projection (FBP), it is more computationally intensive and requires longer processing time. (Koetzier et al., 2023).[3]

IR Techniques Variants

i. Algebraic Reconstruction Technique (ART): The first iterative reconstruction technique used in CT was developed by Hounsfield. It refines images by minimizing the difference between measured and calculated projections. (Ginthör, S. J., et. al., 2020) [7]

ii. Iterative Sparse Asymptotic Minimum Variance: A parameter-free iterative method for super-resolution tomographic reconstruction, based on compressed sensing, applicable in CT, MRI, and synthetic-aperture radar. (Guido, G., et al., 2023). [10]

iii. Statistical Reconstruction: This method consists of five components: an object model, a system model, a statistical model, a cost function, and an iterative algorithm. It frequently employs Poisson statistics and regularization techniques to enhance image quality (Guido, G., et al., 2023). [10]

iv. Learned Iterative Reconstruction: Integrates machine learning techniques with traditional information retrieval methods, such as convolutional neural networks. This combination usually leads to faster and higher-quality reconstructions. (Guido, G., et al., 2023). [10]

v. Model-Based Iterative Reconstruction (MBIR): This method enhances image quality by reducing noise and artifacts, though it may lead to a "plastic" look and longer reconstruction times. (Koetzier et al., 2023).[3]

vi. Hybrid Iterative Reconstruction (HIR): This approach confidently integrates FBP with MBIR, effectively striking a balance between speed and image quality, and is widely recognized as state-of-the-art. (Koetzier et al., 2023). [3]

vii. High Order Multi Directional Total Variation (HOM-TV): Concentrates on preserving edge details while reducing noise and streak artifacts, resulting in quicker reconstruction times. (Bai et al., 2024). [14]

- Deep Learning Image Reconstruction (DLIR): Neural networks boost the image quality by tumbling noise and artifacts. Deep Learning Image Reconstruction (DLIR) methods significantly enhance traditional techniques in low-dose CT by using large training datasets. Their effectiveness relies on the quality of this data while emerging technologies like photon-counting CT promise further advancements. Dual-domain learning, which analyzes both sinogram and image data, helps improve reconstruction accuracy. (Quan, Yan., et al., 2023). [8]

- DL-MLEM-IR-UNET-ESRGAN: Integrates deep learning filters with the Maximum Likelihood Expectation Maximization (ML-EM) algorithm and ESRGAN, significantly enhancing image quality while reducing reconstruction time. (Pham, M. et al., 2024). [15]

- Score Matching and Maximum a Posteriori (MAP) Estimation: A deep learning approach utilizes the score function from Bayesian statistics to enhance image reconstruction from sparse data, ensuring convergence and producing high-quality images from sparse-view CT data. (Chang, M. et al., 2022). [9] [16] IR techniques improve upon FBP's

Volume 38 No. 5s, 2025
ISSN: 1311-1728 (printed version); ISSN: 1314-8060 (on-line version)

limitations by integrating models of the CT scanning process and utilizing prior knowledge of image characteristics. These methods enhance image quality at lower radiation doses, although they are still computationally intensive and may produce images that appear "plastic." (Koetzier et al., 2023) [3] IR is useful in applications that require dose reduction, such as pediatric imaging and oncologic evaluations. (Guido, G. et al., 2023). [10]

- Machine Learning and Block Coordinate Descent (ML-BCD): Combines ML for parameter calibration with block coordinate descent for image reconstruction, particularly useful in portable CT systems with unknown geometry parameters (Kawashima H. et al., 2022). [11].

- Hybrid Supervised-Unsupervised Learning: Integrates model-based image reconstruction with neural networks, optimizing the reconstruction process through a fixed-point iteration framework. This approach is effective in low-dose CT scenarios with limited training data (Minghan et al., 2022). [12]

- Deep Learning and Sparse Modelling: A hybrid framework that combines supervised DL with unsupervised sparse modeling to handle low-dose CT reconstruction effectively (Minghan et al., 2022). [12]

- Sparse View CT: Reduces X-ray exposure time, necessitating methods to suppress noise and artifacts. To overcome these obstacles, Fast IR algorithms have been created., achieving high-fidelity images quickly (Bai et al., 2024).[14]

- Noise Reduction Techniques: Techniques like TrueFidelity (TF) and Advanced intelligent Clear-IQ Engine Body Sharp (AC) offer different noise reduction strategies with varying effectiveness in uniform and non-uniform regions (Kawashima H. et. al., 2022). [11] Studies comparing DLIR techniques with FBP have shown that DLIR can significantly reduce noise while preserving image details. Different DLIR methods vary in their noise reduction strategies, with some prioritizing edge preservation over noise filtering (Tshetiz et al., 2023). [13]

While deep learning (DL) and hybrid methods have advanced CT image reconstruction, challenges persist, including the need for large training datasets, instability, and limited generalizability across different conditions. Native methods: filtered back projection (FBP) and iterative reconstruction (IR) remain relevant due to their simplicity and established use, despite some limitations in low-dose applications. New methods are continuing to evolve to meet diverse imaging needs. (Quan, Yan., et al., 2023).[8]

OBJECTIVES

Related Work

Koetzier L. et al. (2023) discuss CT image reconstruction techniques including FBP, MBIR, HIR, and DLIR. FBP struggles with noise in low-dose imaging, while MBIR enhances quality but requires longer reconstruction times. Hybrid methods combine FBP and MBIR for improved performance. Depending on training data quality, DLIR uses AI for faster, higher-quality images from lower doses. [3]

Received: August 08, 2025

ISSN: 1311-1728 (printed version); ISSN: 1314-8060 (on-line version)

Ikuta, M. et al. (2022) detail that FBP is fast and effective with high X-ray doses but has issues with low-dose imaging due to increased stochasticity. IR utilizes a Bayesian approach, incorporating a CT scanning model and prior knowledge of image quality. The paper introduces "GRU reconstruction," a novel neural network that employs dual-domain learning and a new backpropagation algorithm (BPTS) to improve reconstruction performance.[2]

Kawashima H. et al. (2022) compare GE's TF and Canon's AC DLIR techniques against FBP using water-bath and textured phantoms. TF offers moderate noise reduction while maintaining original signals, whereas AC specializes in noise filtering, particularly at low doses and high reduction strength.[11]

Guido, G. et al. (2023) Compare FBP and advanced IR algorithms, it was concluded that using backward or both backward and forward projections in low-dose CT datasets can improve image quality. These iterative techniques are essential for routine workflows and quantitative imaging, helping to reduce radiation exposure in oncologic patients while addressing the limitations of traditional methods.[10]

Wright, C. (2022) explored an image reconstruction technique using the Filtered Back Projection (FBP) algorithm based on the Radon transform for CT images. It achieved a high Structural Similarity Index Measure (SSIM) of 0.9839 and a Mean Squared Error (MSE) of 0.0002. The research considered the impact of different projections, filters, and cut-off frequencies on reconstruction quality, highlighting the need for further investigation into advanced filters and interpolation methods.[5]

Cong, W., et. al., (2023) present a deep learning method for image reconstruction from MAP estimation in CT, aimed at improving sparse low-dose CT images, which often suffer from loss of detail and artifacts. Unlike traditional analytic algorithms, this approach ensures convergence in the iterative reconstruction process by utilizing the score function from Bayesian statistics, enhancing the quality of sparse-view CT images.[16]

Bai, L. et al. (2024) present an efficient IR algorithm that reduces streak artifacts and noise in CT images. The HOM-TV method enhances reconstruction by preserving edges and using non-local means, resulting in high-quality images from quickly acquired data, with an SSIM value of 0.9755 and a reconstruction time of 36 seconds.[14]

Pham, C. T., et al. (2024) introduce a CT image reconstruction method, DL-MLEM-IR-UNET-ESRGAN, which combines the ML-EM algorithm with deep learning techniques like CNN, UNet, and ESRGAN. This approach achieves an average SSIM of 0.9980 and PSNR of 53.2119, while also reducing reconstruction time.[15]

Anam, C., et al., (2023) compare two CT image reconstruction techniques: Adaptive Statistical Iterative Reconstruction (ASIR-V) and Deep Learning Iterative Reconstruction (DLIR). ASIR-V reduces noise at varying strengths, while DLIR enhances noise texture and preserves sharpness. Using noise power spectrum (NPS) and modulation transfer function (MTF) for evaluation, the study finds that DLIR offers superior noise reduction at low frequencies without compromising spatial resolution.[17]

Received: August 08, 2025

Volume 38 No. 5s, 2025
ISSN: 1311-1728 (printed version); ISSN: 1314-8060 (on-line version)

Zhang, C. et al., (2024) present XTransCT, a novel CT image reconstruction technique using a Transformer architecture that reconstructs images from two ultra-sparse X-ray projections. This approach significantly enhances speed and image quality, achieving a 300% increase in reconstruction speed compared to traditional 3D convolution methods, processing images in about 44 ms per 3D reconstruction.[18]

Yan, Q. et al. (2023) CT image reconstruction techniques have transitioned from traditional to advanced AI-based approaches. While conventional methods optimize only one aspect of image quality, AI aims to generate superior images quickly and with abridged radiation exposure. However, challenges like the need for large datasets and limited generalizability persist.[8]

Kyung, D. et al. (2023) present PerX2CT, a novel CT reconstruction technique using perspective projection from two perpendicular X-ray images. This method efficiently reconstructs 3D CT slices by extracting local and global features while minimizing radiation exposure. Leveraging deep learning, PerX2CT addresses the challenges of estimating 3D structures from limited 2D data, showing excellent performance in clinical applications.[19]

Chaudhary, S. K., et al., (2022) explore X-ray CT image reconstruction techniques, focusing on the Algebraic Method (AM) and the Multiplicative Algebraic Reconstruction Technique (MART). While AM has a low-cost setup, it faces slow convergence and high memory demands. MART maximizes image entropy but typically uses square grids. A modified polar grid approach is proposed to enhance MART by reducing reconstruction time and storage requirements and optimizing projection coefficient calculations for fan-beam geometry in 2D reconstruction.[20]

Meng, C. et al. (2022) CT image reconstruction techniques include block coordinate descent (BCD) algorithms, which optimize unknown geometry parameters and the image concurrently. The proposed hybrid machine learning and BCD (ML-BCD) approach enhances parameter calibration and image reconstruction accuracy by mapping sinogram data to geometry parameters using a machine learning model. This method improves upon traditional BCD and machine learning techniques by refining initial guesses for geometry parameters, leading to more accurate reconstructions in the presence of experimental errors.[21]

Trotta, L., et al., (2022) compare two CT image reconstruction techniques: ray-driven and voxel-driven back-projection. The ray-driven approach, based on Siddon's algorithm, is less effective for small geometries. In contrast, the voxel-driven technique, using bilinear interpolation, offers better results with less noise and fewer artifacts. An IR algorithm called OSC-TV is also utilized, improving image quality, especially for small regions of interest (ROIs).[22]

Al-Ola, et. al., (2022) explore infrared techniques for CT, highlighting the maximum-likelihood expectation maximization (MLEM) and simultaneous multiplicative algebraic reconstruction technique (SMART). It introduces a new algorithm, OS-MART, which combines ordered subsets expectation-maximization (OS-EM) with MART using hybrid

Received: August 08, 2025

ISSN: 1311-1728 (printed version); ISSN: 1314-8060 (on-line version)

means or weighted geometric. This approach aims to improve reconstruction quality and speed up convergence, enhancing image quality and reducing noise in CT imaging.[23]

Sato, H., et. al., (2023) discuss deep learning techniques for enhancing high-contrast CT images. Improved spatial resolution and reduced noise significantly enhance image clarity and detail compared to traditional methods, as demonstrated using phantom models.[24]

Zhong, X. et al., (2023) presents a novel CT image reconstruction technique that combines sparsity regularization with deep learning. It utilizes deep residual networks and L0-norm minimization for improved resolution, optimized using the alternating direction method. Results demonstrate better signal-to-noise ratio and detail recovery in simulated and real CT images.[25]

Eulig, E., et. al., (2022) examine CT image reconstruction techniques, emphasizing iterative reconstruction (IR) methods that incorporate prior knowledge. It discusses advancements in deep learning approaches that surpass traditional CT denoising methods, while also addressing concerns about the interpretability, robustness, and safety of these neural networks and the need for post-hoc interpretation during reconstruction. [26]

Brady, S. L. (2023) discuss CT image reconstruction techniques: IR, FBP, and DLR. DLR reduces noise magnitude without significantly changing texture, aligning more with FBP. It shows potential for greater dose reductions of 44% to 83%, exceeding the typical 15-30% reduction for IR. [27]

Kawashima, H., et. al., (2022). The paper evaluates dual deep-learning image reconstruction techniques, TF and AC, against FBP using a water bath and a textured phantom. It highlights that TF offers moderate noise reduction in non-uniform areas while preserving original signals. In contrast, AC focuses on filtering noise, especially at low doses and higher reduction levels.[11]

Zhang, M. et al., (2022). CT image reconstruction techniques, including conventional methods like FBP and IR, have limitations in low-dose applications. Reconstruction periods will be shortened and image quality will be enhanced by future developments. A systematic review highlights that deep learning methods enhance noise suppression, reduce artifacts, and preserve structures, leading to better low-dose image quality.12]

Lu, K., Ren, L., et al. (2022) review CT image reconstruction techniques, including the conventional filtered back projection (FBP) method, fully connected deep learning (FCDL), and geometry-guided deep learning (GDL). It introduces a novel approach called multi-beamlet deep learning (GMDL), which uses smaller fully connected layers to enhance projection-to-image transformation. GMDL improves image quality in low-dose CT reconstructions while reducing model size and GPU memory requirements compared to FCDL and GDL.[28]

Zhang, Z., et. al., (2022). The paper presents a Directional Total Variation (DTV) algorithm for reconstructing images in phase-contrast computed tomography (PCCT) from limited angular range (LAR) data. Unlike existing methods that focus on boundary images, the DTV algorithm reconstructs the refractive index distribution through an optimization approach

International Journal of Applied Mathematics
Volume 38 No. 5s, 2025
ISSN: 1311-1728 (printed version); ISSN: 1314-8060 (on-line version)

with DTV and non-negativity constraints. The study finds that the two-orthogonal-arc configuration produces more accurate reconstructions with fewer artifacts than the single-arc setup.[29]

Problem Statement with Motivation of Work

FBP is effective at high radiation doses but struggles with noise and artifacts in low-dose imaging (Cong, W. et al., 2024) [4]. On the other hand, the image quality generated by IR is much better, but the computational time intensively increases the computation cost. (Koetzier et al., 2023).[3]. This debate leads to the requirement of new techniques that claim to be as fast as FBP and as effective as IR.

METHODS

Mathematical Concept: The continued framework is used in the reconstruction theory where techniques are derived analytically, even though the CT projections are inherently discrete. The complexity of discrete sampling is addressed in the ultimate development of the reconstruction algorithm. For clarity, a few transforms were applied in a continuous domain.

Radon Transform: For ease of explanation & understanding, the 2D (a,b) plane is considered, and the source/detector prearrangement rotates about the object (Figure 2).

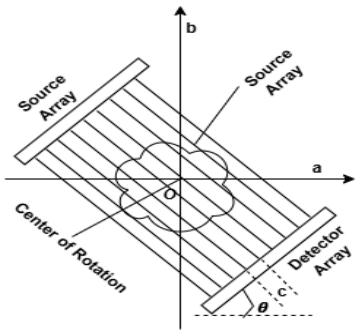

Figure 2 Parallel-beam projection q(c, θ) with parallel-beam structure.

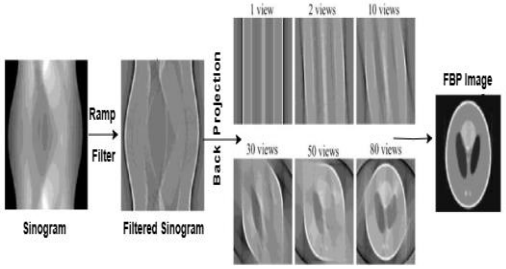

Figure 3 Filtered Back Projection.

Dirac's delta (δ) function effectively isolates the specific sections of the object that are penetrated by X-rays, allowing for precise analysis and enhanced clarity in imaging. It's important to remember that the delta function, δ(i) = 0 universally except at i equal to 0, where it becomes infinitely large. Additionally, the delta function satisfies the shifting property for the real-valued g(a) function.

$$g(a_0) = \int_{-\infty}^{\infty} g(a)\,\delta(a - a_0)da \quad \ldots\ldots\ldots\ldots (1)$$

A parallel projection at detector element s with rotation angle θ of the source/detector array can be expressed as follows:

$$q(c,\theta) = \iint_{-\infty}^{\infty} f(a,b)\delta(a\cos\theta + b\sin\theta - c)dadb \quad \ldots\ldots\ldots\ldots\ldots (2)$$

Received: August 08, 2025

International Journal of Applied Mathematics
Volume 38 No. 5s, 2025
ISSN: 1311-1728 (printed version); ISSN: 1314-8060 (on-line version)

The f(a,b) signifies the attenuation coefficient of X-ray for any object at the location (a,b). The delta (δ) function chooses the c= a cos θ + b sin θ line, which joins the source and detector array at c with θ as the rotation. The expression q(c, θ) represents an integral along this line, measured on the detector. The procedure for transforming functional values f(a,b) as integral values for line q(c, θ) is known as the two-dimensional Radon transformation. The vital challenge in CT image reconstruction lies in calculating the functional values f(a,b) back from the evaluated line integral values q(c,θ); known as the inverse of Radon transformation. An essential concept of CT image reconstruction is the technique known as back-projection, which will be explored in greater depth. Back projection acts as a conjugate process to forward projection, though it should be noted that it is not an inverse process. In the realm of X-ray parallel beam projections, back-projection meticulously assigns to each point (a, b) in the object coordinates the integral r(a, b), which represents the accumulation of projection values corresponding to the X-rays traversing that specific point (a, b). This method allows for the reconstruction of images by blending information gathered from multiple angles, thereby providing a comprehensive view of the internal structure being analyzed.

$$r(a,b) = \int_0^{\pi} \quad q(c,\theta)|_{c=a\,cos\theta+b\,sin\theta}\, d\theta$$
……. (3)

Filtered Back Projection

The inverse Fourier transform is used to demonstrate the derivation of FBP as follows:

$$f(a,b) = \int_{-\infty}^{\infty} \quad \int_{-\infty}^{\infty} \quad F(u,v)e^{2\pi i(ua+vb)}dudv$$
……. (4)

Then it will be written as polar coordinates Fpolar (ω, θ)

$$f(a,b) = \int_0^{\pi} \quad \int_{-\infty}^{\infty} \quad F_{polar}(\omega,\theta)|\omega|e^{2\pi i\omega(a\,cos\theta+b\,sin\theta)}d\omega d\theta$$
……. (5)

Conferring from the Fourier Slice Theorem,

$$f(a,b) = \int_0^{\pi} \quad \int_{-\infty}^{\infty} \quad q(\omega,\theta)\ |\omega|\ e^{2\pi i\omega(a\,cos\theta+b\,sin\,\theta)}\ d\omega\ d\theta$$
……. (6)

It elaborates on a pivotal product within one-dimensional Fourier space, denoted as q(ω, θ), along with the absolute value of ω, represented as |ω|. The inverse Fourier transform of the product q(ω, θ) · |ω| establishes a direct relationship to a convolution operation in the spatial domain, effectively linking frequency information to spatial arrangements. To meticulously define the inverse Fourier transform of |ω|, the filter kernel j(c) is employed, which acts as a crucial tool in the analysis. As a result, in the spatial domain, the preceding equation can be articulated with clarity and precision as follows:

$$f(a,b) = \int_0^{\pi} \quad q(c,\theta) * j(c)|_{c=a\,cos\theta+b\,sin\theta}\, d\theta$$
……. (7)

Received: August 08, 2025

International Journal of Applied Mathematics
Volume 38 No. 5s, 2025
ISSN: 1311-1728 (printed version); ISSN: 1314-8060 (on-line version)

It represents the back projection of q(c, θ) convoluted with j(c).

Algorithm: FBP

Step 1: For every θ angle, calculate the one-dimensional Fourier transform of q(c, θ) regarding s, gaining q(ω, θ).

Step 2: qk`(ω, θ) = q(ω, θ) · Hl,α,β,wk(ω) with k=0, 1,…, 10.

Step 3: Perform one-dimensional inverse Fourier transform of qk`(ω, θ) concerning ω, obtaining qk`(c, θ) with k=0, 1, …, 10.

Step 4: Calculate q`(c, θ) by leasing q`(c, θ) = qk(c, θ) if q(c, θ) is approximately equal to 0.1 · k · qmax.

Step 5: Back project q`(c, θ) to acquire the ultimate image.

Problem Formulation

To improve FBP image quality at low-dose imaging, the FBP must be assisted with other emerging techniques. It may better result in low-dose imaging, it will be a milestone in detecting the problem even in low-intensity projection to minimize radiation exposure to the patient body.

Novelty

This research changes the filter kernel j(c)|c= $a\,cos\theta + b\,sin\theta$ used in the FBP with altered-filter kernel j(c)|c= $a\,cos\theta + b\,sin\theta + absin\theta cos\theta$. After the image generated from FBP is provided to self-tuned CNN.

Experimental Hybrid Model

The proposed hybrid model for CT image reconstruction underwent a comprehensive evaluation using the well-established NIH-AAPM-Mayo Clinic CT Grand Challenge dataset. This dataset comprises CT images with a uniform slice thickness of 3 mm, totaling 2,378 images derived from ten distinct patients with varying clinical profiles. The images were meticulously divided into training and testing datasets to optimize model performance. The training dataset encompasses 1,923 images from eight patients, while the testing dataset contains 455 images from the remaining two patients, allowing for a robust assessment of the model's capabilities. The original images are defined by dimensions of 150 × 150 pixels, providing sufficient resolution for detailed analysis. Importantly, the focal point of the X-ray source is strategically positioned 541 mm from the isocenter of the imaging field. A factor that significantly enhances the overall precision and clarity of the resulting images. The imaging setup employs a well-calibrated geometry, with a specified distance of 949.15 mm from the X-ray detector to the source. This configuration features 888 detector elements, each with a precise measurement of 1.024 mm, facilitating the capture of high-quality projections. To further refine the imaging process, we implemented a distance-driven algorithm during the simulation of X-ray CT imaging, which not only improves efficiency but also enhances the accuracy of the generated images. For the creation of few-view projection datasets, we employed a total of 90 projection views that are systematically

Received: August 08, 2025

International Journal of Applied Mathematics
Volume 38 No. 5s, 2025
ISSN: 1311-1728 (printed version); ISSN: 1314-8060 (on-line version)

distributed throughout a full 360-degree rotation, ensuring comprehensive coverage of the scanned volume. Additionally, to authentically replicate real-world X-ray imaging conditions for tomographic image reconstruction, we deliberately introduced Poisson noise into the projection datasets, reflecting the inherent variability in clinical imaging scenarios. This approach ensures that the model is robust and well-equipped to handle the complexities of actual imaging environments.

A hybrid model is proposed and compared with SART variants. In the proposed model, FBP is sequentially merged with the modified CNN having three 2D convolution layers having 32 filters of size 3*3 kernels, 64 filters of size 3*3 kernels, and 128, 3*3 size kernels filters, with Rectified Linear Unit (Relu) as the activation function on an input of shape 150*150 in a batch size of 8, along with three 2D max-pooling layers with a pool size of 2*2 kernels. Each block works in a feed-forward fashion. The flatten function is applied, before applying the dense layer (128, activation='relu') to the outcome of the previous steps. The dropout with a 0.5 value was taken to overcome the overfitting in the model. Softmax is used in the close-fitted dense layer as the activation function at the output layer. The model is expertly compiled with the powerful ADAM optimizer and leverages categorical cross-entropy as the loss function, ensuring optimal performance and accuracy. The training process is performed on a machine with NVIDIA GEFORCE RTX GPU of 6 GB memory.

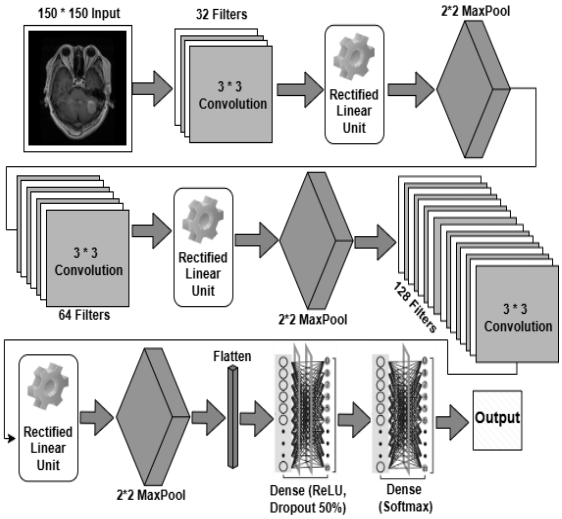

Figure 4 Proposed CNN Architecture

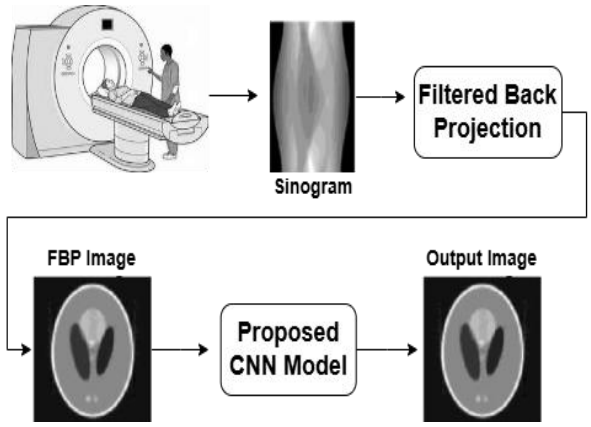

Figure 5 Work Flow of Proposed Hybrid Technique

The model was fitted by applying 15 epochs and callbacks as early stopping and model checkpoint. Data augmentation and preprocessing for the proposed model include rescaling to 1.0/255, 20 degrees rotation range, shift ranges for height and width is 0.2, also 0.2 shear range, along with 0.2 zoom range, horizontal flip set to True, and nearest as fill mode. Firstly, while doing FBP reconstruction, the input images will be converted into grayscale images. Then, circular masking is performed by putting zero values outside the circular region, resulting in a masked image blurred outside the circular fringe from the center to the size of its radius. Then, radon transformation is applied to get a sinogram from the grayscale image with theta value ranging from 0 to 180 degrees. Inverse radon transformation is used in the next step to reconstruct the image with appropriate theta values and a “ramp” filter. In the

Received: August 08, 2025

International Journal of Applied Mathematics
Volume 38 No. 5s, 2025
ISSN: 1311-1728 (printed version); ISSN: 1314-8060 (on-line version)

end, the cvtColor function from OpenCV is used to convert the grayscale reconstructed image to RGB.

RESULTS

Image reconstructions were performed from 90 projection datasets using the standard FBP, SART, SART with total variation (TV) regularization, and the proposed FBP algorithms. Figure 4 presents the images reconstructed from the above methods.

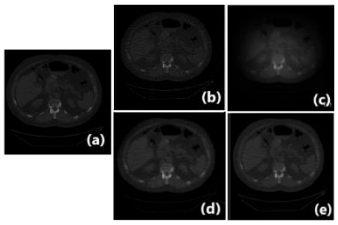

Figure 6 Comparison of reconstructed images using existing and proposed methods. (a) True Image, (b) the image reconstructed from 90 projections using FBP, (c) the image reconstructed from 90 projections using the SART iteration, (d) the image reconstructed from 90 projections using the SART iteration with total variation minimization (e) the image reconstructed from 90 projections using the proposed r-FBP.

For a comprehensive evaluation of image quality, this experiment employs two prominent measures: Peak Signal-to-Noise Ratio (PSNR) and Structural Similarity Index Measure (SSIM). PSNR quantitatively analyzes the discrepancies in pixel values between the original reference image and its degraded version, meticulously focusing on absolute errors to highlight variations. Conversely, SSIM provides a more nuanced assessment by examining the structural patterns, contrast levels, and brightness characteristics of both images, enabling a deeper understanding of perceptual differences. Together, these methodologies offer a thorough and insightful perspective on image quality assessment.

$$PSNR = 10 * log_{10}\left(\frac{P_{max}^2}{\frac{1}{mn}\sum_{i=0}^{m-1}\sum_{j=0}^{n-1}[I(i,j)-N(i,j)]^2}\right) \quad \ldots\ldots\ldots\ldots\ldots (8)$$

Pmax is the maximum pixel value, I(m*n) is a noise-free image, N is a noisy approximation of I(m*n),

$$SSIM\ (x,y) = \frac{(2\mu_x\mu_y + c_1)(2\sigma_{xy} + c_2)}{(\mu_x^2+\mu_y^2+c_1)(\sigma_x^2+\sigma_y^2+c_2)} \quad \ldots\ldots\ldots\ldots\ldots (9)$$

μ_x the pixel sample mean of x, μ_y the pixel sample mean of y, σ_x^2 the sample variance of x, σ_y^2 the sample variance of y, σ_{xy} the sample covariance of x and y, $c_1 = (0.01 * (2^{bits\ per\ pixel} - 1))^2$, $c_2 = (0.03 * (2^{bits\ per\ pixel} - 1))^2$

Table 1: Quality metric of the reconstructed image.

	r-FBP	FBP	SART	SART+ TV

Received: August 08, 2025

Volume 38 No. 5s, 2025
ISSN: 1311-1728 (printed version); ISSN: 1314-8060 (on-line version)

SSIM	0.7916	0.3703	0.5406	0.6724
PSNR	19.0424	11.8587	16.797	17.1514

CONCLUSION & FUTURE WORK

The proposed hybrid method showcases remarkable performance in preserving structural information, particularly in intricate texture features. It achieves exceptional spatial and contrast resolution and effectively minimizes image noise, resulting in clearer and more detailed visuals. The Peak Signal-to-Noise Ratio (PSNR) and Structural Similarity Index Measure (SSIM) were critical metrics to evaluate the reconstructions of sparse-view images. Impressively, the learning-based reconstruction method achieves an average PSNR of 19.0424 dB and an SSIM of 0.7916, which significantly exceed the results of traditional reconstruction techniques, as illustrated in Table 2. Moreover, the integration of innovative image generative transformers—such as Diffusion Vision Transformers, Microsoft's StyleSwin (a cutting-edge transformer-based Generative Adversarial Network), OpenAI's DALL·E, Vision Transformers (ViT), and Imagen—unlocks vast potential for transformative breakthroughs in this rapidly evolving field.

REFERENCES

[1] Griffin, J., (2022, June). Computed Tomography. National Institute of Biomedical Imaging and Bioengineering, An official website of the United States government. https://www.nibib.nih.gov/science-education/science-topics/computed-tomography-ct (accessed on Nov,15. 2024)

[2] Ikuta, M., & Zhang, J. (2023, December). A Deep Convolutional Gated Recurrent Unit for CT Image Reconstruction. IEEE Transactions on Neural Networks and Learning Systems, 34(12) PP. 10612-10625. https://doi.org/10.1109/TNNLS.2022.3169569.

[3] Koetzier, L. R., Mastrodicasa, D., Szczykutowicz, T. P., van der Werf, N. R., Wang, A. S., Sandfort, V., van der Molen, A. J., Fleischmann, D., & Willemink, M. J. (2023). Deep Learning Image Reconstruction for Computed Tomography: Technical Principles and Clinical Prospects. Radiology, 306(3), e221257. https://doi.org/10.1148/radiol.221257.

[4] Cong, W., Xia, W., & Wang, G. (2024). Tomographic Image Reconstruction Using an Advanced Score Function (ADSF). ArXiv, arXiv:2306.08610v7.

[5] Wright, C. (2022). Image Reconstruction Technique Using Radon Transform (pp. 735–754). https://doi.org/10.1007/978-981-19-1577-2_55.

[6] Vamvakeros, A. (2017). Operando chemical tomography of packed bed and membrane reactors for methane processing (Doctoral dissertation, UCL (University College London)).

Received: August 08, 2025

ISSN: 1311-1728 (printed version); ISSN: 1314-8060 (on-line version)

[7] Ginthör, S. J., Schlagnitweit, J., Bechmann, M., & Müller, N. (2020). Nuclear spin noise tomography in three dimensions with iterative simultaneous algebraic reconstruction technique (SART) processing. Magnetic Resonance, 1(2), 165-173.

[8] Quan, Yan., Yunfan, Ye., Jing, Xia., Zhiping, Cai., Zhilin, Wang., Qiang, Ni. (2023). AI-Based Image Reconstruction for Computed Tomography: A Survey. 36(3):2545-2558. doi: 10.32604/iasc.2023.029857.

[9] Chang, Meng., James, G., Nagy. (2022). Numerical methods for CT reconstruction with unknown geometry parameters. Numerical Algorithms, 92(1):831-847. doi: 10.1007/s11075-022-01451-3).

[10] Guido, G., Polici, M., Nacci, I., Bozzi, F., De Santis, D., Ubaldi, N., ... & Caruso, D. (2023). Iterative reconstruction: State-of-the-art and future perspectives. Journal of Computer-Assisted Tomography, 47(2), 244-254.

[11] Kawashima, H., Ichikawa, K., Takata, T., & Seto, I. (2022). Comparative Assessment of Noise Properties for Two DLCT Image Reconstruction Techniques and Filtered Back Projection. Medical Physics, 49(10), 6359–6367. https://doi.org/10.1002/mp.15918.

[12] Minghan, Zhang., Saikun, Gu., Yuhui, Shi. (2022). The use of DL methods in low-dose computed tomography image reconstruction: a systematic review. Complex & Intelligent Systems, 8(6):5545-5561. doi: 10.1007/s40747-022-00724-7.

[13] Tshetiz, Dahal., Bimal, Nepal. (2023). Evaluation of image resolution and quantification parameters on fdg-pet/ct images in patients with metastatic breast cancer using Q. clear and osem reconstruction techniques. Indian journal of anatomy and surgery of head, neck, and brain, 9(3):83-90. doi: 10.18231/j.ijashnb.2023.017.

[14] Bai, L., Du, Y., & Long, C. (2024). CT image reconstruction via industrial CT fast scanning. Journal of Instrumentation, 19(03), P03009.

[15] Pham, C. T., Tran, T. T. T., Huynh, D., Nguyen, Q. C., & Nguyen, T. H. (2024). CT image reconstruction: integrating iterative methods with Ml-EM algorithm and deep learning models. Cybernetics and Physics, 13(2), 130–141. https://doi.org/10.35470/2226-4116-2024-13-2-130-141

[16] Cong, W., Xia, W., & Wang, G. (2023). Image Reconstruction from Sparse Low-Dose CT Data via Score Matching. arXiv preprint arXiv:2306.08610.

[17] Anam, C., Hidayanto, E., Sutanto, H., Naufal, A., & Dougherty, G. (2023). Comparison of noise-power spectrum and modulation-transfer function for CT images reconstructed with iterative and DLimage reconstructions: An initial experience study. Polish Journal of Medical Physics and Engineering, 29(2), 104–112. https://doi.org/10.2478/pjmpe-2023-0012.

[18] Zhang, C., Liu, L., Dai, J., Liu, X., He, W., Chan, Y., & Liang, X. (2024). XTransCT: ultra-fast volumetric CT reconstruction using two orthogonal x-ray projections for

ISSN: 1311-1728 (printed version); ISSN: 1314-8060 (on-line version)

image-guided radiation therapy via a transformer network. Physics in Medicine & Biology, 69(8), 085010.

[19] Kyung, D., Jo, K., Choo, J., Lee, J., & Choi, E. (2023, June). Perspective projection-based 3d CT reconstruction from biplanar X-rays. In ICASSP 2023-2023 IEEE International Conference on Acoustics, Speech and Signal Processing (ICASSP) (pp. 1-5). IEEE.

[20] Chaudhary, S. K., Wahi, P., & Munshi, P. (2022). Modified Polar Grid-based Accelerated Image Reconstruction Technique for X-ray CT. E-Journal of Nondestructive Testing, 27(12). https://doi.org/10.58286/27520.

[21] Meng, C., & Nagy, J. G. (2022). Numerical methods for CT reconstruction with unknown geometry parameters. Numerical Algorithms, 92(1), 831–847. https://doi.org/10.1007/s11075-022-01451-3.

[22] Trotta, L., Matenine, D., Martini, M., Lemarechal, Y., Francus, P., & Després, P. (2022). On the use of voxel-driven back projection and iterative reconstruction for small ROI CT imaging. 7th International Conference on Image Formation in X-Ray Computed Tomography, 12304, 123042V. https://doi.org/10.1117/12.2647012.

[23] Al-Ola, O. M., Kasai, R., Yamaguchi, Y., Kojima, T., & Yoshinaga, T. (2022). Image Reconstruction Algorithm Using Weighted Mean of Ordered-Subsets EM and MART for Computed Tomography. Mathematics, 10(22), 4277. https://doi.org/10.3390/math10224277.

[24] Sato, H., Fujimoto, S., Tomizawa, N., Inage, H., Yokota, T., Kudo, H., Fan, R., Kawamoto, K., Honda, Y., Kobayashi, T., Minamino, T., & Kogure, Y. (2023). Impact of a Deep Learning-based Super-resolution Image Reconstruction Technique on High-contrast Computed Tomography: A Phantom Study. Academic Radiology. https://doi.org/10.1016/j.acra.2022.12.040.

[25] Zhong, X., Liang, N., Cai, A., Yu, X., Li, L., & Yan, B. (2023). Super-resolution image reconstruction from sparsity regularization and deep residual-learned priors. Journal of X-Ray Science and Technology. https://doi.org/10.3233/XST-221299.

[26] Eulig, E., Ommer, B., & Kachelrieß, M. (2022). Reconstructing invariances of CT image denoising networks using invertible neural networks. 7th International Conference on Image Formation in X-Ray Computed Tomography, 12304, 123040S. https://doi.org/10.1117/12.2647170

[27] Brady, S. L. (2023). Implementation of AI image reconstruction in CT- how is it validated, and what dose reductions can be achieved. British Journal of Radiology, 20220915. https://doi.org/10.1259/bjr.20220915

[28] Lu, K., Ren, L., & Yin, F.-F. (2022). A geometry-guided multi-beamlet deep learning technique for CT reconstruction. Biomedical Physics & Engineering Express, 8(4), 045004. https://doi.org/10.1088/2057-1976/ac6d12

ISSN: 1311-1728 (printed version); ISSN: 1314-8060 (on-line version)

[29] Zhang, Z., Chen, B., Xia, D., Sidky, E. Y., Anastasio, M., & Pan, X. (2022). Image reconstruction in phase-contrast CT with shortened scans. In 7th International Conference on Image Formation in X-Ray Computed Tomography (Vol. 12304, pp. 505-511). SPIE.

[30] Apostol T, Mathematical Analysis, 2nd ed.: Addison Wesley, 1974.

Received: August 08, 2025